Electronic Supplementary Material (ESI) for ChemComm.

Ni_3S_2@MoO_3 core/shell arrays on Ni foam modified with Ultrathin CdS layer as a superior electrocatalyst for hydrogen evolution reaction

Preparation of CdS-MoO_3/Ni_3S_2/NF

A simple microwave hydrothermal method was used to prepare the MoO_3/Ni_3S_2 on the Ni foam substrate. In a typical reaction, firstly, Ni foam was ultrasonically cleaned in 3M HCl, acetone, ethanol and deionized (DI) water for 20 min each, respectively, prior to use. And then, a 2*4 cm^2 area of the Ni foam substrate was placed vertically at the bottom of a microwave reactor (CEM, MARS 6 240/50, USA) (100ml) and immersed in 30mL aqueous solution composing of 0.1g of P123 (a triblock copolymer, HO $(CH_2CH_2O)_{20}(CH_2CH(CH_3)O)_{70}(CH_2CH_2O)_{20}H$), 0.27mmol of Ni（$NO_3$）$_2$·$6H_2O$, 0.27mmol of $(NH_4)_6Mo_7O_{24}\cdot 4H_2O$ and 1.2 mmol of $C_3H_7NO_2S$. After microwave irradiation at 220°C for 1hour, the as-prepared sample of the MoO_3/Ni_3S_2 on Ni foam structure (labeled MoO_3/Ni_3S_2/NF) was then removed from the solution, and washed thoroughly with distilled water. The loading mass of MoO_3/Ni_3S_2 grown on the Ni foam was ~3.47 mg cm^{-2}, which was calculated from the weight increment of Ni foam after catalyst preparation. Significantly, the precursor of $Ni(NO_3)_2$ $6H_2O$ is extra added in the reaction for purpose of the reduction in consumption of Ni foam. Over consumption of Ni foam for Ni_3S_2 will produce more defects on Ni substrate, and thus leading to poor electric conduction. As for the control experiment to synthesize MoO_3/Ni_3S_2 nanorod arrays on Ni foam without extra addition of Ni precursor(labelled MoO_3/Ni_3S_2//NF), the process was carried out via the similar microwave hydrothermal method except that $Ni(NO_3)_2$ $6H_2O$ is absent.

For preparation of CdS modifying MoO_3/Ni_3S_2/NF (labeled CdS-MoO_3/Ni_3S_2/NF), the as prepared MoO_3/Ni_3S_2/NF was immersed in the aqueous solution of 10mM $CdCl_2\cdot 2.5H_2O$ and 2mM $Na_2S_2O_3$, followed by electrodeposition via. Cyclic voltammetry (CV). During the electrodeposition, HCl was used to adjust the electrolyte, and the pH value of the electrolyte prepared is at ~1.52. The experiment was carried out using a CHI 660E electrochemical analyzer with a three-electrode cell, in which the as prepared MoO_3/Ni_3S_2/NF (2cm*3cm), a saturated calomel electrode (SCE) and Pt sheet (2.5 cm*1 cm) served as the working electrode, reference electrode and counter electrode, respectively. The CV for control samples was conducted 2 cycles at 70°C, respectively, with scanning rate of $5mVs^{-1}$ and in the voltage range of -0.9 to -0.3 V. And then the composite film was rinsed by deionized water, and dried. The loading mass of CdS on MoO_3/Ni_3S_2/NF for sample of CdS-MoO_3/Ni_3S_2/NF was evaluated at 0.0017 mg cm^{-2} from the weight increment after electrodeposition. Another control sample of Ni_3S_2 loaded on NF (indicated as Ni_3S_2/NF) is prepared by similar process with that of MoO_3/Ni_3S_2/NF except that MoO_3precursor is rule out. Ni foam foil covered with CdS (labeled CdS-NF) and Ni_3S_2 covered with CdS (labeled CdS-Ni_3S_2/NF) is obtained using similar electrodeposition process in which NF or Ni_3S_2/NF was immersed in the aqueous solution of 10mM $CdCl_2\cdot 2.5H_2O$ and 2mM$Na_2S_2O_3$. All these control samples related to Ni_3S_2 are prepared with the extra addition of $Ni(NO_3)_2$.

Materials characterization

The morphologies of the samples were investigated by scanning electron microscopy (SEM JEOL-6701F) and high resolution transmission electron microscopy (HRTEM JEOL JSM-3010). The chemical composition of samples was analyzed by X-ray photoelectron spectroscopy (Thermo Scientific Escalab 250Xi). Thermo instrument and all peak positions were normalized to the binding energy of C 1s (285eV). The molecular vibration mode and defect of samples were measured by Raman spectra (Lab Ram HR800). X-ray diffraction (XRD) patterns were obtained using a Rigaku D/max-2500B2+/PCX system which is operated at 40 kV and 30 mA using Cu Kα radiation at a scan rate of 4°min^{-1}.

Electrochemical measurements

Electrochemical experiments were performed in a three-electrode cell made of quartz. A carbon rod and calomel were used as the counter and reference electrodes, respectively, and the as prepared samples were employed as the working electrode with an area of 0.25 cm^2. Linear sweep voltammetry (LSV) with scan rate of 1mV s^{-1} was conducted in 1M KOH solution（pH=14）using an electrochemical workstation

(CHI660E, Chenhua, China). Potentials were referenced to an RHE by adding 1.067 V (0.241+ 0.059×pH) in 1 M KOH.As for control samples of Pt/C, the catalysts (5mg) were first dispersed in a mixture of 0.5 mL ethanol and 10μL nafion solution, respectively. And then the dispersion was ultrasonicated for 30 min to form a homogeneous ink and then loaded onto a preprocessed 0.25 cm^2 NF by drop-coating, in which loading mass for Pt/C was kept consistent with that of the as prepared products. Prior to the test measurements, N_2 was introduced into the electrolyte solution to eliminate the dissolved oxygen. All of the potentials in the LSV polarization curves were IR-corrected with respect to the Ohmic resistance of the solution. Electrochemical impedance spectroscope measurements(EIS) were carried out at -0.2V (HER) vs. RHE in the frequency range of 10^{-1} to 10^4 Hz. Electrochemical capacitance measurements were determined using cyclic voltammetry for two cycles between 0.1 and 0.2 V vs. RHE with scanning rates of 60, 80, 100,120 and 150 mVs^{-1}. Conventional Hall measurements (Phys Tech RH2030) were conducted in air at room temperature on 1 cm^2 samples.

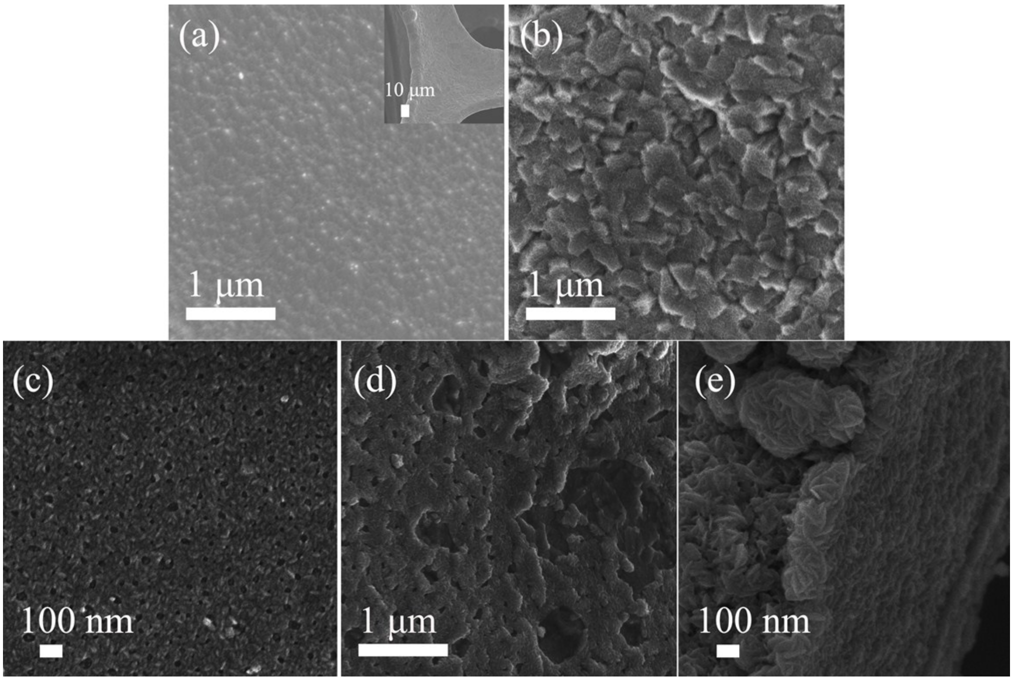

Figure S1 The SEM images of top views for (a) Ni foam, (b) Ni_3S_2/NF, (c) CdS-NF, (d) CdS-Ni_3S_2 /NF, and (e) the cross section of CdS-MoO_3/ Ni_3S_2 /NF.

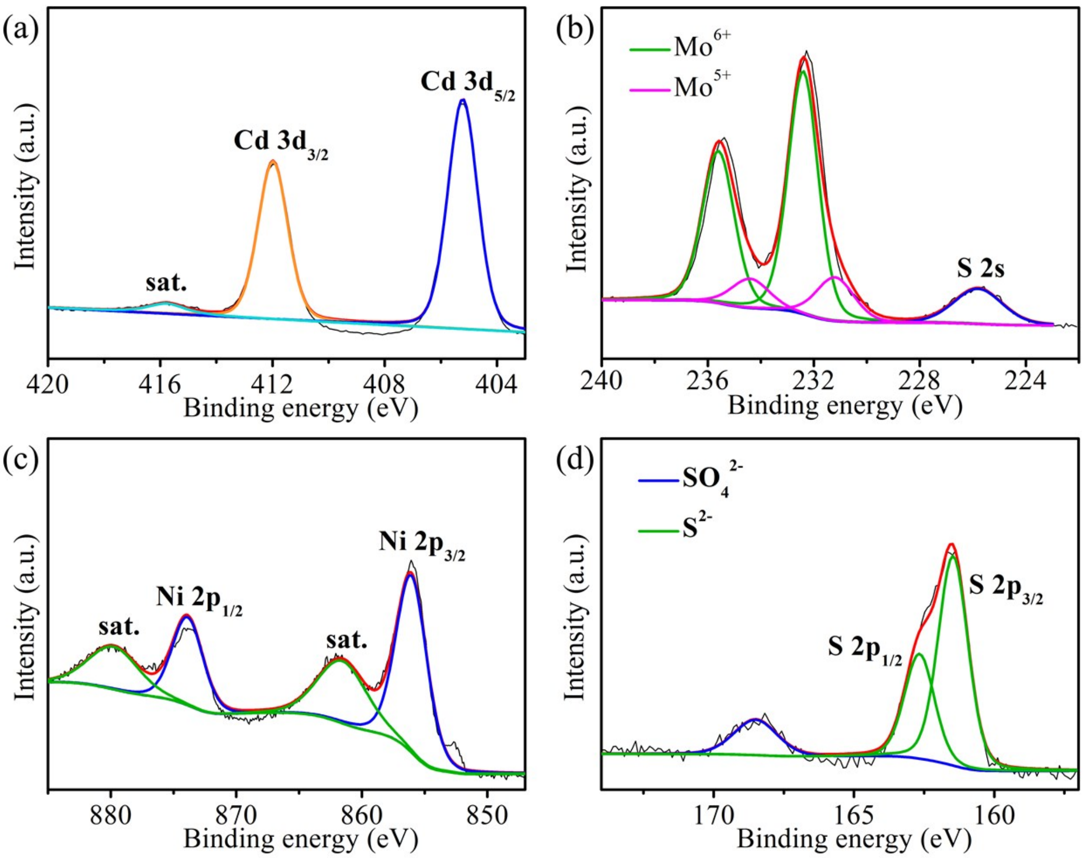

Figure S2 High resolution XPS spectrum of (a) Cd3d, (b) Mo3d, (c) Ni2p, and (d) S2p

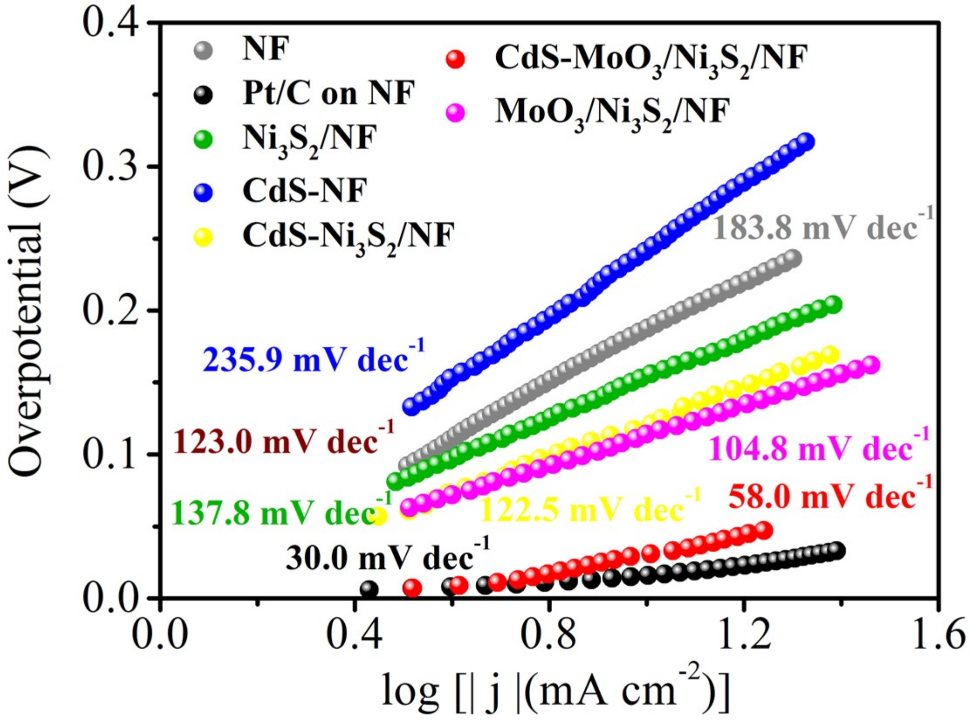

Figure S3 Tafel plots of the as prepared samples. The control experiments are conducted in 1 M KOH. The scanning rate is 1mVs^{-1}

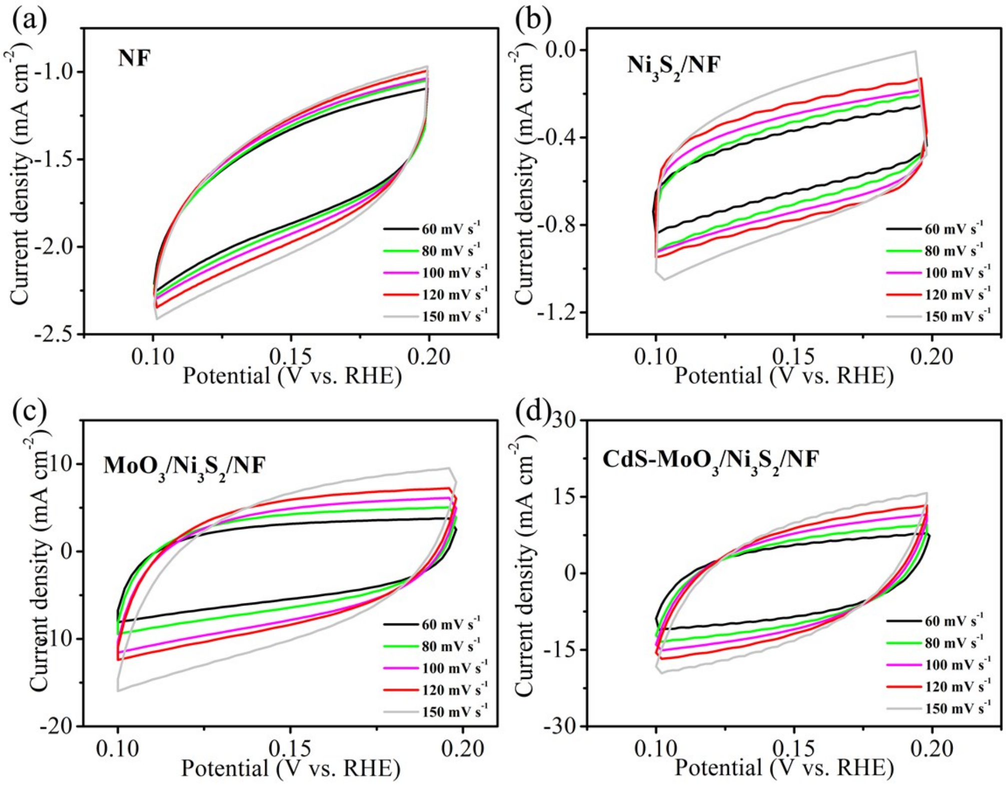

Figure S4 EDLC measurements of (a) NF, (b) Ni_3S_2/NF, (c) MoO_3/Ni_3S_2/NF and (d) CdS-MoO_3/Ni_3S_2/NF

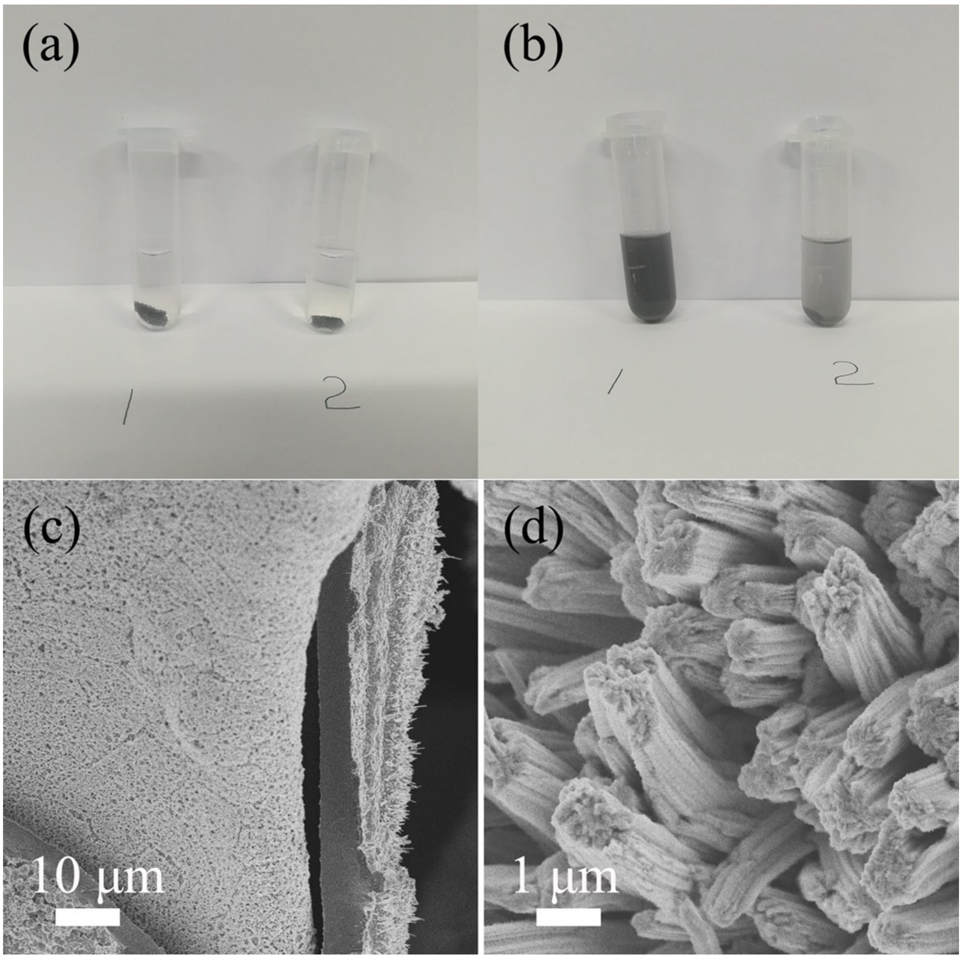

Figure S5 MoO_3/Ni_3S_2/NF with Ni foam as only Ni source (left, labeled 1), MoO_3/Ni_3S_2 //NF with extra addition of Ni $(NO_3)_2$ (right, labeled 2) in 2mL alcohol, (a) before and (b) after ultrasonic treatment for 20 min, and SEM images of MoO_3/Ni_3S_2/NF with Ni foam as only Ni source with the magnification of (c) ×1000 and (d) ×10000.

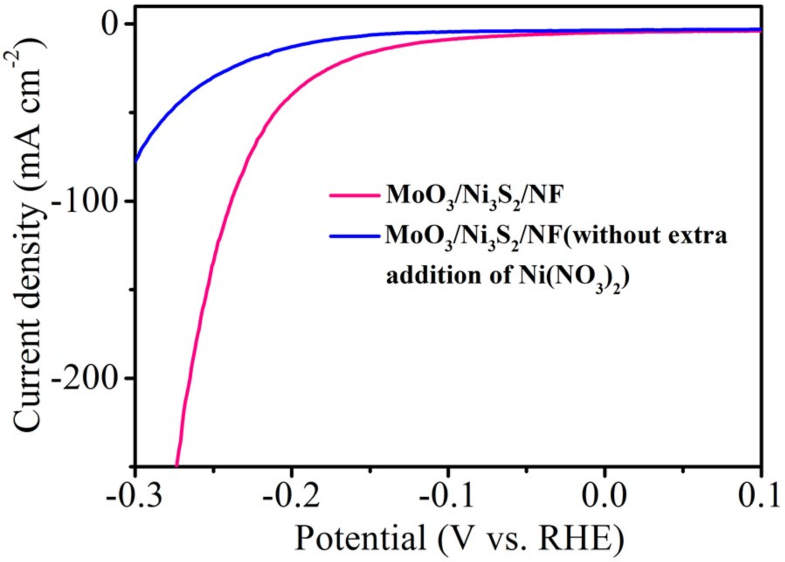

Figure S6 J−V curves of cathodic polarization of MoO_3/Ni_3S_2/NF with and without Ni precursor addition

In the case of extra addition of Ni $(NO_3)_2$, the CdS-MoO_3/Ni_3S_2/NF nanoarrays are continuously grown and solidly anchored on the NF substrate due to the decreased consumption of Ni foam during the formation of Ni_3S_2

(Fig.S1e). $MoO_3/Ni_3S_2/NF$ prepared with Ni foam as only Ni source displays a wrapping, peeling and cracking morphology on which the much thick rod arrays are grown. The adhesion or stability of the catalyst anchored on substrate is compared through ultrasonically treating the $MoO_3/Ni_3S_2/NF$ samples with or without the extra addition of Ni $(NO_3)_2$ (sample2 and sample1, respectively in Fig.S5a and S5b). After ultrasonic treatment, the dispersion of sample 2 is still kept transparent in contrast to that of sample1 (Fig.S5b), indicating that MoO_3/Ni_3S_2 /NF with extra addition of Ni $(NO_3)_2$ is firmly anchored on the substrate. Fig.S6 confirmed that the electrocatalytic activity of $MoO_3/Ni_3S_2/NF$ with Ni precursor addition was better than its control counterpart.

The resistances of the as prepared samples were determined by conventional Hall measurements, and the resistances for MoO_3/Ni_3S_2 /NF (sample2) and CdS-MoO_3/Ni_3S_2 /NF are 4.70 and 2.84, respectively, indicating the appropriate integration of highly active sites with ultrafast electron transfer features can greatly enhance the electrical property of the CdS-$MoO_3/Ni_3S_2/NF$ electrocatalyst.

Table S1 Comparison of resistance of as prepared samples☆measured by Hall measurement

Sample resistance	Ni_3S_2 /NF	CdS-Ni_3S_2 /NF	MoO_3/Ni_3S_2//NF (sample 1)	MoO_3/Ni_3S_2/NF （sample2）	CdS-MoO_3/Ni_3S_2 /NF
Rho (Ohm*cm)	$6.94*10^{-7}$	$6.97*10^{-7}$	$7.37*10^{9}$	$4.70*10^{-7}$	$2.84*10^{-7}$

☆:All the as prepared samples except MoO_3/Ni_3S_2//NF (sample1) are prepared with the extra addition of $Ni(NO_3)_2$.

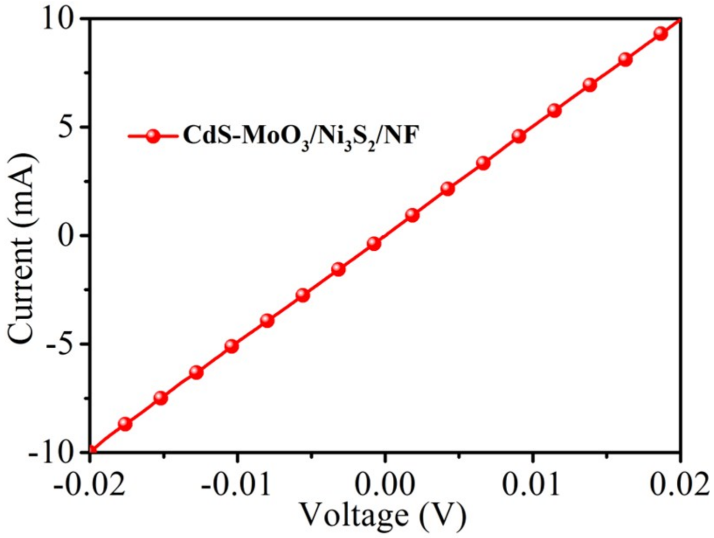

Figure S7 I–V characteristics measured for sample CdS-$MoO_3/Ni_3S_2/NF$ (The I-V characteristics was measured on an solar cell test system (XES-70S1, SAN-EI ELECTRIC Japan)

In order to demonstrate the electrical transport behavior of CdS-$MoO_3/Ni_3S_2/NF$, the contacts between probes and the specimen were also examined at room temperature. I – V characteristics measured for sample CdS-$MoO_3/Ni_3S_2/NF$ is shown in Fig.S7. The linear behavior of I-V characteristics confirms the Ohmic contact between the probe and the samples. It is observed that CdS-$MoO_3/Ni_3S_2/NF$ is still characterized by conductor behavior in spite of the introduction of CdS semiconductor.

Table S2 Comparisons of HER performances in 1M KOH solution for CdS-MoO_3/Ni_3S_2/NF nanoarray electrodes with other HER electrocatalysts

Catalysts	**η_{10} (mV)**	**Tafel Slope (mV dec^{-1})**	**Electrolyte**	**Ref. (Year)**
CdS-MoO_3/Ni_3S_2/NF	30	58	1.0 M KOH	This work
P-MoO_{3-x} nanosheet	166	42	0.5 m H2SO4,	1(2017)
MoS_2–Ni_3S_2 HNRs	98	61	1.0 M KOH	2(2017)
CdS/Ni_3S_2/PNF	121	110	1.0 M KOH	3(2017)
N-$MoSe_2$/VG	98	49	0.5 M H_2SO_4	4(2017)
$Ni_{0.89}Co_{0.11}Se_2$ MNSN	85	52	1.0 M KOH	5(2017)
CoP@NC	129	58	1.0 M KOH	6(2017)
MoO_3/NF	140	56	0.1 M KOH	7(2016)
MoO_x/Ni_3S_2/NF	106	--	1.0 M KOH	8(2016)
Ni_5P_4	150	--	1.0 M KOH	9(2016)
MoS_{2-} Ni_3S_2 heterostructure	110	83.1	1.0 M KOH	10(2016)
$NiCo_2S_4$ NW/NF	210	58.9	1.0 M KOH	11(2016)
Ni_3S_2–MoS_2 interlaced nanoflakes/Ti	--	70	1.0 M KOH	12(2016)
3D porous $NiSe_2$/Ni	143	49	0.5MH_2SO_4	13(2016)

REFERENCES

1 L. Li, T. Zhang, J. Yan, X. Cai and S. Liu, *Small*, 2017, **13**, 1700441.

2 Y. Yang, K. Zhang, H. Lin, X. Li, H. C. Chan, L. Yang and Q. Gao, *ACS Catal.*, 2017, **7**, 2357-2366.

3 S. Qu, J. Huang, J. Yu, G. Chen, W. Hu, M. Yin, R. Zhang, S. Chu and C. Li, *ACS Appl. Mat. Interfaces*, 2017, 29660-29668.

4 S. Deng, Z. Yu, Y. Zeng, Y. Wang, Z. Yao, Y. Fan, S. Lin, X. Wang, X. Lu and X. Xia, *Adv. Mater.*, 2017, **29**, 1700748.

5 B. Liu, Y. F. Zhao, H. Q. Peng, Z. Y. Zhang, C. K. Sit, M. F. Yuen, T. R. Zhang, C. S. Lee and W. J. Zhang, *Adv. Mater.*, 2017, **29**, 1606521.

6 F. Yang, Y. Chen, G. Cheng, S. Chen and W. Luo, *Acs Catal.*, 2017, **7**, 3824-3831.

7 Z. Luo, R. Miao, T. D. Huan, I. M. Mosa, A. S. Poyraz, W. Zhong, J. E. Cloud, D. A. Kriz, S. Thanneeru and J. He, *Adv. Energy Mater.* , 2016, **6**, 1600528.

8 Y. Wu, G. D. Li, Y. Liu, L. Yang, X. Lian, T. Asefa and X. Zou, *Adv. Funct. Mater.*, 2016, **26**, 4839-4847.

9 M. Ledendecker, H. Schlott, M. Antonietti, B. Meyer and M. Shalom, *Adv. Energy Mater.*, 2016, **7**, 1601735.

10 J. Zhang, T. Wang, D. Pohl, B. Rellinghaus, R. Dong, S. Liu, X. Zhuang and X. Feng, *Angew. Chem.-Int. Edit.*, 2016, **55**, 6702-6707.

11 A. Sivanantham, P. Ganesan and S. Shanmugam, *Adv. Funct. Mater.*, 2016, **26**, 4661-4672.

12 T. An, Y. Wang, J. Tang, W. Wei, X. Cui, A. M. Alenizi, L. Zhang and G. Zheng, *J. Mater. Chem. A* 2016, **4**, 13439-13443.

13 H. Zhou, Y. Wang, R. He, F. Yu, J. Sun, F. Wang, Y. Lan, Z. Ren and S. Chen, *Nano Energy*, 2016, **20**, 29-36.